



Gravitational and
capillary soil
moisture dynamics

A. Castillo et al.

This discussion paper is/has been under review for the journal Hydrology and Earth System Sciences (HESS). Please refer to the corresponding final paper in HESS if available.

Gravitational and capillary soil moisture dynamics for hillslope-resolving models

A. Castillo^{1,3}, F. Castelli², and D. Entekhabi^{1,3}

¹Department of Civil and Environmental Engineering, Massachusetts Institute of Technology, Cambridge, MA 02139, USA

³Center for Environmental Sensing and Modeling, Singapore-MIT Alliance for Research and Technology, Singapore, Singapore

²Department of Civil and Environmental Engineering, University of Florence, Florence, Italy

Received: 18 June 2014 – Accepted: 21 June 2014 – Published: 30 June 2014

Correspondence to: A. Castillo (aldrichcastillo@gmail.com)

Published by Copernicus Publications on behalf of the European Geosciences Union.

Title Page

Abstract

Introduction

Conclusions

References

Tables

Figures



Back

Close

Full Screen / Esc

Printer-friendly Version

Interactive Discussion



Abstract

Distributed and continuous catchment models are used to simulate water and energy balance and fluxes across varied topography and landscape. The landscape is discretized into plan computational elements at resolutions of 10^1 – 10^3 m, and soil moisture is the hydrologic state variable. At the local scale, the vertical soil moisture dynamics link hydrologic fluxes and provide continuity in time. In catchment models these local scale processes are modeled using one-dimensional soil columns that are discretized into layers that are usually 10^{-3} – 10^{-1} m in thickness. This creates a mismatch between the horizontal and vertical scales. For applications across large domains and in ensemble mode, this treatment can be a limiting factor due to its high computational demand. This study compares continuous multi-year simulations of soil moisture at the local scale using (i) a 1-D version of a distributed catchment hydrologic model; and (ii) a benchmark detailed soil water physics solver. The distributed model uses a single soil layer with a novel dual-pore structure, and employs linear parameterization of infiltration and some other fluxes. The detailed solver uses multiple soil layers and employs nonlinear soil physics relations to model flow in unsaturated soils. Using two sites with different climates (semiarid and sub-humid), it is shown that the efficient parameterization in the distributed model captures the essential dynamics of the detailed solver.

1 Introduction

Soil moisture controls the partitioning of rainfall into infiltration and runoff, and it controls land surface temperature through its effect on the partitioning of available energy into sensible and latent heat fluxes. It is the hydrologic state variable, together with land temperature, in models of surface water and energy balance. The states dynamics are affected by hydrometeorological forcing of precipitation, radiation and atmospheric evaporative demand. Furthermore, topography, landuse, and soil properties

HESSD

11, 7133–7168, 2014

Gravitational and capillary soil moisture dynamics

A. Castillo et al.

[Title Page](#)

[Abstract](#)

[Introduction](#)

[Conclusions](#)

[References](#)

[Tables](#)

[Figures](#)

[⏪](#)

[⏩](#)

[⏴](#)

[⏵](#)

[Back](#)

[Close](#)

[Full Screen / Esc](#)

[Printer-friendly Version](#)

[Interactive Discussion](#)



across the landscape, affect soil moisture temporal evolution (Western and Grayson, 2000; Lawrence and Hornberger, 2007; Vereecken et al., 2007; Ivanov et al., 2010; Liu et al., 2012; Beven and Germann, 2013).

There are diverse methods for measuring soil moisture e.g dielectric- and heat dissipation-based approaches. The suitability of a certain method or system depends largely on the desired scale, accuracy, and resolution, both in space and in time. Unfortunately, all current observing systems have their shortcomings. For instance, in situ sensors can provide high accuracy and fine temporal resolution but at limited spatial footprint; sampling campaigns can provide better spatial resolution and coverage but at low sampling frequency and duration; while space-borne remote sensing platforms provide global spatial coverage for surface soil moisture sensing but at coarse spatial resolution and with infrequent revisits.

Numerical hydrologic models fill some of the shortcomings of observations. Incoming radiation and precipitation are used in conjunction with water and energy balance models to simulate the evolution of soil moisture in the vadose zone and estimate the water and energy fluxes across the landscape. Harter and Hopmans (2004) describes how hydrologic models have traditionally been used by two largely disconnected groups: the watershed hydrologists (and recently also climate modelers) who deal with macro-processes; and the soil physicists who study soil properties and states at the laboratory or local to plot scales. Watershed hydrologists have traditionally used lumped or semi-distributed models that treat the vadose zone as a zero-dimensional black box. The computational timestep is usually hourly, daily, or even longer. Two examples of heritage models used by watershed hydrologists are the semi-distributed models TOP-MODEL (Beven and Kirby, 1979) and SAC-SMA (Burnash et al., 1973) which have both been demonstrated as highly capable in simulating streamflow. Meanwhile, soil physicists who have detailed measurements of soil properties and states at the local to plot scales, model unsaturated flow by discretizing the hydrologically active soil column into layers that are usually 10^{-3} to 10^{-1} m in thickness, and using the Richards equation which can be written as,

Gravitational and capillary soil moisture dynamics

A. Castillo et al.

[Title Page](#)

[Abstract](#)

[Introduction](#)

[Conclusions](#)

[References](#)

[Tables](#)

[Figures](#)

[⏪](#)

[⏩](#)

[◀](#)

[▶](#)

[Back](#)

[Close](#)

[Full Screen / Esc](#)

[Printer-friendly Version](#)

[Interactive Discussion](#)



$$\frac{\partial \theta}{\partial t} = -\frac{\partial}{\partial z} \left[K(\theta) \left(\frac{\partial \psi}{\partial z} + 1 \right) \right] \quad (1)$$

where, K is the hydraulic conductivity, ψ pressure head, z elevation with respect to a datum, θ soil moisture, and t time. For stability, this nonlinear partial differential equation is solved using sub-hourly time steps.

Over the years, the modeling efforts of the two disciplines have started to converge as manifested by the emergence of physically-based distributed hydrologic models (DHMs). These models discretize the landscape in computational elements that are 10^1 to 10^3 m in the horizontal. Adopting the practice in soil physics, many DHMs employ Richards equation and discretize the hydrologically active soil layer into vertical layers that are 10^{-3} to 10^{-1} m in thick. Some DHMs that use the Richards formulation include MIKE-SHE (Refsgaard and Storm, 1995) and ParFlow (Ashby and Falgout, 1996) that use grids for horizontal discretization; and PIHM (Qu and Duffy, 2007) and TRIBS (Ivanov et al., 2004) that use triangulated irregular network (TIN) as horizontal elements (see Table 1). More DHMs are discussed by Smith et al. (2004, 2012) under the context of the Distributed Model Intercomparison Project. There are example studies that demonstrate the advantages of DHMs over lumped and semi-distributed model (Bartholomes and Todini, 2005; Castelli et al., 2009; Smith et al., 2004; Vieux et al., 2004). Although promising, the use of DHMs has its own challenges and criticisms which include (i) the need for a high number of inputs that often should have fine spatiotemporal resolutions; (ii) the use of many parameters which makes the calibration process tedious and raises the concern on equifinality (Beven, 2006); and (iii) the high computational requirement (Smith et al., 2004, 2012).

The hydrologically active soil mantle is but a thin layer draped over the landscape, and it serves as the intermediate water storage connecting the surface above and the deeper soil layers or groundwater aquifer below. Because of the horizontal-to-vertical scale disparity, DHMs often treat flow dynamics in the soil as one-dimensional i.e., lateral subsurface flow is considered negligible. Exceptions include MIKE-SHE and

Gravitational and capillary soil moisture dynamics

A. Castillo et al.

[Title Page](#)

[Abstract](#)

[Introduction](#)

[Conclusions](#)

[References](#)

[Tables](#)

[Figures](#)



[Back](#)

[Close](#)

[Full Screen / Esc](#)

[Printer-friendly Version](#)

[Interactive Discussion](#)



**Gravitational and
capillary soil
moisture dynamics**

A. Castillo et al.

[Title Page](#)[Abstract](#)[Introduction](#)[Conclusions](#)[References](#)[Tables](#)[Figures](#)[Back](#)[Close](#)[Full Screen / Esc](#)[Printer-friendly Version](#)[Interactive Discussion](#)

ParFlow which can be setup to solve the full 3–D Richards equation. This treatment is however very computationally intensive as demonstrated by Kollet et al. (2010) who utilized 16 384 processors to achieve reasonable run time for ParFlow simulations of a basin on the order of 10^3 km^2 at fine spatial resolution (10^0 to 10^1 m in the horizontal and 10^{-2} to 10^{-1} m in the vertical).

Models based on Richards formulation are useful when the vertical profile of soil moisture is desired especially when the soil column is significantly heterogeneous. However, information about the vertical soil structure is often not available and highly uncertain where available.

Based on the foregoing discussion, the scales mismatch between the vertical and horizontal discretization of DHMs (millimeters to centimeters in the vertical soil column vs. tens to hundreds of meters in the horizontal) leads to two main problems: (1) solving the local scale vertical soil moisture dynamics based on Richards equation is computationally demanding; and (2) such fine vertical discretization increases the number of parameters to calibrate, and state variables to initialize.

Moreover, although Richards equation is probably an appropriate model for unsaturated flow at the local scale, it is questionable whether it is an appropriate physical model for watershed and large scale applications (Beven, 1995; Harter and Hopmans, 2004; Beven and Germann, 2013). Also, using this equation for plan elements that are in the order of 10^1 – 10^3 m, makes the implicit assumptions that the vertical dynamics of soil moisture at the local scale is scale-invariant (up to the limit of the plan element area). To the contrary, field measurements show that soil hydraulic conductivity and pore properties related to the soil retention curve (of ψ) vary significantly both in the horizontal and vertical (Gelhar et al., 1992; Rubin, 2003; Zhang et al., 2004). Furthermore, the review paper of Beven and Germann (2013) argues that the use of Richards equation to model field soil should not be considered physics-based but rather a convenient conceptual approximation. They explain that the Darcy and Richards equations have dominated soil physics in the last few decades because of the ready availability of numerical models based on these formulations, despite the convincing evidence that

**Gravitational and
capillary soil
moisture dynamics**

A. Castillo et al.

[Title Page](#)[Abstract](#)[Introduction](#)[Conclusions](#)[References](#)[Tables](#)[Figures](#)[Back](#)[Close](#)[Full Screen / Esc](#)[Printer-friendly Version](#)[Interactive Discussion](#)

their underlying assumptions, and carefully controlled experimental setups, are inappropriate for natural conditions. They highlighted the importance of macropores and suggested the use of soil structure with at least two flow pathways. Models that use such structure are the 1-D model of Gerke and van Genuchten (1993), the 1-D model MACRO (Larsbo et al., 2005), and the 1-D or 2-D/3-D model HYDRUS (Šimůnek and van Genuchten, 2008). In these three models, the soil column is composed of a macropore and a matric compartment, with the water flow in the matric compartment still solved using Richards equation.

The inclusion of macropore pathways is dependent on available direct and indirect information on their density and connectivity across the basin. The matric compartment still needs to be characterized in distributed models. In this study we focus on a novel dual-pore parameterized approach to this compartment. We compare the performance of the approach to a benchmark detailed Richards equation solver. The aim of the dual-pore parameterized approach is to capture the essential dynamics of the matric compartment moisture relations while remaining efficient for applications in distributed hydrologic models (possibly even in ensemble mode). The pore space is divided into gravity and capillary components that each control different set of hydrologic fluxes and the two are themselves connected. The partitioning allows the capture of two different time scales in the local scale soil moisture processes.

In this study we test the fidelity of the novel approach to modeling the soil moisture state in a distributed hydrologic model. The Modello Bilancio Idrologico Distribuito e Continuo (MOBIDIC) is a physically-based and raster-distributed catchment hydrologic model that solves mass and energy balance simultaneously. Table 1 lists the features of MOBIDIC, and compares it with some of the hydrologic models that have been mentioned. A key feature of MOBIDIC is its use of a single layer of soil with dual compartments – one for gravitational water and another for capillary-bound water. This representation accounts for both fast and slow processes. At the same time, it makes the model computationally efficient. Furthermore it reduces the number of state variables in the overall dynamic modeling system.

Gravitational and capillary soil moisture dynamics

A. Castillo et al.

[Title Page](#)

[Abstract](#)

[Introduction](#)

[Conclusions](#)

[References](#)

[Tables](#)

[Figures](#)



[Back](#)

[Close](#)

[Full Screen / Esc](#)

[Printer-friendly Version](#)

[Interactive Discussion](#)



Division of hillslope soil water into storage that drains under gravitational force and storage that is held under capillary action has been used in diverse applications. The concept of field capacity – variably-defined as it may be (drainage after 3 days or water content at a given potential) – has been used in agronomy and irrigation applications.

Gravitational water can be considered stored water in the soil above its field capacity. Gravitational water contributes to lateral exchange and vertical percolation fluxes. It also can fill smaller pores that hold water under capillary action. Capillary water is stored water below the field capacity and can be defined to be limited to water above the residual content. Plant roots and evaporation in general can remove capillary water. Thus gravitational and capillary water dynamics affect different hydrologic fluxes. More recently, Brooks et al. (2009) used water isotope data in a humid catchment field experiment to also distinguish between “tightly-bound water” that is used by trees and mobile water that participates in “translatory flow” and enters streams. The conceptualization of the soil matrix into a dual-pore structure with each storage affecting different hydrologic fluxes has been further suggested as a general framework for characterizing hydrologic and ecohydrological response (McDonnell, 2014). White and Toumi (2012) modify a land-surface model to adopt the tightly-bound and mobile water parameterization that also each affect different hydrologic fluxes. In this study we use the gravitational and capillary dual-pore approach to modeling soil moisture dynamics in a hillslope-resolving distributed hydrologic model. We test the fidelity of this approach to local processes by comparing its soil moisture dynamics with that resulting from a numerical model that solves the vertical heat and moisture dynamics using detailed physics including (Eq. 1).

The goal of this paper is to demonstrate that MOBIDIC which has a dual-pore structure, can simulate the dynamics of depth-averaged soil moisture as effectively as models using multiple soil layers and Richards equation. In addition, since most of the previous applications of MOBIDIC assessed its performance based mainly on stream-flow which is an area-integrated flux, this study also demonstrates that MOBIDIC is

capable of correctly simulating the dynamics of soil moisture, soil temperature, and evapotranspiration (ET).

The paper begins with a description of the catchment hydrologic model MOBIDIC, and a description of its 1-pixel version which is used in this particular study. This is followed by an overview of the selected benchmark model which is the legacy 1-D SHAW. Then the correspondence between SHAW and MOBIDIC variables, the measures of model performance, and the two study sites, are described.

2 Methods

2.1 The distributed hydrologic model MOBIDIC

2.1.1 Overview

The Modello Bilancio Idrologico Distribuito e Continuo (MOBIDIC) is a physically-based and raster-distributed catchment hydrologic model that solves mass and energy balance simultaneously. It was developed by Castelli et al. (2009) for basin-scale catchment modeling. This study introduces some modifications to the original parameterization. MOBIDIC uses a single layer for each plan element or soil unit. To account for the different roles of gravity and capillary forces in moving and storing soil water, each soil unit has dual compartments: a gravity reservoir composed of large pores that drain under gravity, and a capillary reservoir composed of smaller pores that do not drain under gravity and hold water under capillary action. This representation gives the model computational parsimony.

MOBIDIC is composed of several MATLAB™ subroutines. Pre-processing of topographic and geomorphologic model inputs, e.g., pit-filling of digital elevation model (DEM), determination of flow directions, computation of flow accumulation, and delineation of the river network and the basin boundary, is done in ArcGIS™ using the Hydrology Toolbox. Other required model inputs are land cover and soil maps, which

HESSD

11, 7133–7168, 2014

Gravitational and capillary soil moisture dynamics

A. Castillo et al.

[Title Page](#)

[Abstract](#)

[Introduction](#)

[Conclusions](#)

[References](#)

[Tables](#)

[Figures](#)



[Back](#)

[Close](#)

[Full Screen / Esc](#)

[Printer-friendly Version](#)

[Interactive Discussion](#)



are in turn used to derive parameters such as albedo, turbulent heat exchange coefficient (neutral), canopy interception capacity, and soil hydraulic properties. The model can output time series of streamflow at any point along the river network, and the hydrologic fluxes (e.g., infiltration, runoff, and ET) and states (e.g., soil temperature and water content of the soil capillary and gravity reservoirs) at any point in the basin. More details about MOBIDIC can be found in Campo et al. (2006) and Castelli et al. (2009).

2.1.2 Mass and energy balance

A schematic diagram of MOBIDIC's mass balance for a typical soil unit (on a hillslope) is shown in Fig. 1, where, d is the thickness [L] of the modeled soil layer, z depth [L] below surface (positive downward); and z_w depth [L] to groundwater table. There are four water reservoirs: the dual soil reservoirs (gravity and capillary reservoirs), the plant or canopy reservoir, and the surface for ponds and depressions. The per unit area volume capacities [L] of these reservoirs are denoted by $W_{c,max}$, $W_{g,max}$, $W_{p,max}$ and $W_{s,max}$, and the water content states are W_c , W_g , W_p and W_s , respectively. The water holding capacity of the dual soil reservoirs are parameterized as,

$$W_{g,max} = d(\theta_{sat} - \theta_{fld}) \quad (2)$$

$$W_{c,max} = d(\theta_{fld} - \theta_{res}) \quad (3)$$

where, θ_{sat} , θ_{fld} , and θ_{res} are the volumetric soil moisture [-] at saturation, field capacity, and residual content, respectively. The parameters θ_{sat} , θ_{fld} , and θ_{res} are initialized based on soil texture type and using typical values reported by Rawls et al. (1982).

Within each computational timestep, dt [T], the hydrologic fluxes [$L T^{-1}$] linking elements across the landscape include infiltration–excess runoff R_H , partial-area (saturation from below) runoff R_D , total runoff R_T , return flow R_R , and lateral subsurface flow Q_L . These water fluxes can be limited by the available water to be transported, the allowable transport rate, or the available receiving storage. For each soil moisture storage

Title Page

Abstract

Introduction

Conclusions

References

Tables

Figures

⏪

⏩

◀

▶

Back

Close

Full Screen / Esc

Printer-friendly Version

Interactive Discussion



unit, the allowable rate of infiltration I , absorption Q_{as} from W_g to W_c , percolation Q_{per} , and lateral subsurface flow Q_L , are formulated according to Eqs. (4) to (7),

$$I = \min \{ W_s / dt, K_s, (W_{g,max} - W_g) / dt \} \quad (4)$$

$$Q_{as} = \min \{ W_g / dt, \kappa (1 - W_c / W_{c,max}) \} \quad (5)$$

$$Q_{per} = \begin{cases} \min \{ \gamma W_g, [W_g + (\frac{z_w}{d} - 1) W_{g,max}] / dt \} & \text{if } z_w \geq 0 \\ \min \{ (W_{g,max} - z_w - W_g) / 2 dt, (W_{g,max} - W_g) / dt \} & \text{if } z_w < 0 \end{cases} \quad (6)$$

$$Q_L = \beta W_g \quad (7)$$

where, K_s is the soil saturated hydraulic conductivity [$L T^{-1}$]; and κ , γ , and β are rate coefficients [$1/T$]. The subscripts “up” and “down” denote incoming flow from upstream cell(s), and outgoing flow to downstream cell, respectively; and $Q_{L,bypass}$ and $R_{T,bypass}$ [$L T^{-1}$] are the portions of the lateral subsurface and total surface runoff from upstream cells that are routed directly to the downstream cell.

Infiltration fills the gravity storage at a rate limited by K_s . Absorption flux Q_{as} draws water from gravity storage into available capillary storage. The parameter κ is a linear rate coefficient. The water in gravity storage is lost to percolation or to lateral subsurface flow. Both are again characterized by linear rate coefficients γ and β . κ , γ , and β are dimensionless parameters with values from 0 to 1. For fine soil texture, typically κ is close to 1 since the capillary reservoir is filled first before any substantial filling of the gravity reservoir. Meanwhile, based on comparison of Eq. (6) with the analytic percolation equation of Eagleson (1978), a good initialization of γ is $K_s / W_{g,max}$.

The conceptualization of soil water storage as gravity and capillary storage and the flux relations, see Eqs. (4) to (7), constitute the core of the simplified modeling system. Infiltration fills the larger pores increasing gravity storage. Water is moved from the gravity storage into the smaller capillary storage pores. Losses to the groundwater and lateral flow are only from gravity storage. Simple linear rate constants characterize the time scales of these exchanges. This simple representation is based on physical

HESSD

11, 7133–7168, 2014

Gravitational and capillary soil moisture dynamics

A. Castillo et al.

Title Page

Abstract

Introduction

Conclusions

References

Tables

Figures

⏪

⏩

◀

▶

Back

Close

Full Screen / Esc

Printer-friendly Version

Interactive Discussion



considerations and they result in a parsimonious and computationally efficient modeling approach.

The soil capillary water storage unit can also receive water from capillary rise from shallow water table. There are a number of available capillary rise models e.g., Gardner (1958), Eagleson (1978), and Bogaart et al. (2008). They vary primarily based on their parameterization of K_s and the soil matric potential ψ [L] as function of soil moisture. The capillary rise model of Salvucci (1993), shown in Eq. (8) was chosen because unlike other models, it allows direct calculation of the capillary rise Q_{cap} [L T^{-1}] as a function of ψ and the mean distance of the unsaturated soil layer from the water table d_w [L],

$$Q_{\text{cap}} = \frac{[(d_w/\psi_1)^{-n} - (\psi/\psi_1)^{-n}] K_s}{1 + (\psi/\psi_1)^{-n} + (n-1)(d_w/\psi_1)^{-n}} \quad (8)$$

where ψ_1 [L] is the bubbling pressure, and n [-] is the product of the Brooks–Corey pore-size distribution index and pore-size disconnectedness index. Brooks and Corey (1964) is used to compute ψ ,

$$\psi = \psi_1 S^{-1/m}. \quad (9)$$

The effective soil saturation S [-] is computed as,

$$S = (W_c + W_g)/(W_{c,\text{max}} + W_{g,\text{max}}). \quad (10)$$

The evapotranspiration ET has three components: E_1 is evaporation from canopy retention, E_2 is evaporation from free surface water surfaces, and E_3 is evapotranspiration from the soil:

Gravitational and capillary soil moisture dynamics

A. Castillo et al.

Title Page

Abstract

Introduction

Conclusions

References

Tables

Figures

◀

▶

◀

▶

Back

Close

Full Screen / Esc

Printer-friendly Version

Interactive Discussion



$$ET = E_1 + E_2 + E_3 \quad (11)$$

$$E_1 = \min\{W_p/dt, PET\} \quad (12)$$

$$E_2 = \min\{W_s/dt, PET - E_1\} \quad (13)$$

$$E_3 = \min\left\{\frac{W_c}{dt}, \frac{(PET - E_1 - E_2)}{1 + \exp(\xi - 10S)}\right\}. \quad (14)$$

Equation (14) has the form of an S-curve which was chosen because it mimics the nonlinear behavior of actual ET as a function of potential evapotranspiration PET and relative soil saturation S . It uses a single parameter ξ . S is multiplied by 10 for convenience such that ξ takes on non-negative integer values (suggested value: 2 or 3).

Except during a precipitation event and the subsequent draining period, most of the fluxes are inactive. During dry conditions, the only significant fluxes are ET_3 and Q_{cap} . Moreover, if $z_w \gg d$, then $Q_{cap} \approx 0$.

The potential evapotranspiration PET is determined through surface energy balance under potential (energy-limited) conditions as:

$$\rho_w L_v PET = R_n - H - G \quad (15)$$

where, ρ_w density of water, L_v is the latent heat of vaporization, R_n net incoming radiation, H sensible heat flux, and G heat flux into the soil. Upon calculation of actual evaporation through Eqs. (11) to (14), the energy balance is solved again to update the surface temperature state.

The turbulent fluxes are computed according to Eqs. (16) and (17) where, ρ_a is the density of air, C_a heat capacity of air, C_H turbulent heat exchange coefficient, and U wind speed; T_a and q_a are the temperature, and specific humidity of air, respectively; T_s and q_s are the temperature, and specific humidity of the surface (soil and vegetation continuum), respectively.

$$H = \rho_a C_a C_H U (T_s - T_a) \quad (16)$$

$$L E_v = \rho_a L_v C_H U (q_s - q_a). \quad (17)$$

Title Page

Abstract

Introduction

Conclusions

References

Tables

Figures

⏪

⏩

◀

▶

Back

Close

Full Screen / Esc

Printer-friendly Version

Interactive Discussion



The unknown surface temperature T_s and soil heat flux G are estimated using the heat diffusion equation,

$$\rho_s C_s \frac{\partial T}{\partial t} = \frac{\partial}{\partial z} \left(k \frac{\partial T}{\partial z} \right) \quad (18)$$

where, ρ_s is the density, C_s heat capacity, k thermal conductivity, and T temperature of soil; and t is time. Equation (18) is integrated forward in time using a parsimonious 3-point vertical discretization:

$$T(z = 0) = T_s \quad (19)$$

$$T(z = z_d) = T_d \quad (20)$$

$$T(z = z_y) = T_{\text{constant}} \quad (21)$$

where, z_d and z_y are the damping depths of daily, and yearly heatwaves, respectively. The lower boundary condition is a constant temperature T_{constant} roughly equal to the annual mean air temperature. The upper boundary condition is,

$$k \frac{\partial T_s}{\partial z} = -G \approx L E_v + H - R_n. \quad (22)$$

2.2 The SHAW model

The Simultaneous Heat and Water (SHAW) models the transfer of heat, water, and solute within a 1-D vertical profile composed of multi-layered and multi-species plant cover, snow layer, dead plant residue layer, and multi-layered soil. It was first developed by Flerchinger and Saxton (1989) to simulate soil freezing and thawing, but has since undergone numerous modifications and extensions. It is available for free from the USDA Agricultural Research Service (ARS) Northwest Watershed Research Center (NWRC) website (<ftp.nwrc.ars.usda.gov>). It was chosen as the benchmark model for this study because (i) it simultaneously solves mass and energy balance; (ii) it solves

Gravitational and capillary soil moisture dynamics

A. Castillo et al.

Title Page

Abstract

Introduction

Conclusions

References

Tables

Figures



Back

Close

Full Screen / Esc

Printer-friendly Version

Interactive Discussion



Richards equation for soil moisture; and (iii) it has detailed treatment of evapotranspiration (ET).

In SHAW, a soil column is discretized into computational nodes. The fluxes between nodes are solved using implicit finite-difference. The required inputs include general site information (e.g., location, elevation, aspect); parameters for soil, snow, and vegetation; meteorological forcings (precipitation, air temperature, total solar radiation, wind speed, and relative humidity); lower boundary conditions; and initial states for soil moisture and temperature. Optional inputs are time series of water sources or sinks, and time series of vegetation parameters. The latter, which includes canopy height, biomass, leaf diameter, leaf area index (LAI), and effective root depth, are specified in this study.

2.3 Correspondence between SHAW and MOBIDIC variables

In order to compare the soil moisture dynamics between SHAW and MOBIDIC, the parameters used in both models were set as consistently as possible. For example, the surface albedo is the same in both models. Also, the soil water content at saturation of MOBIDIC and the corresponding depth-averaged value of SHAW are the same.

SHAW and MOBIDIC output different state variables. SHAW gives the volumetric soil moisture θ_i [-] at each soil node i , while MOBIDIC gives the equivalent water depth W [L] stored as capillary and gravity water for its single soil layer. To allow comparison, the results of the two models were converted to depth-averaged soil moisture $\bar{\theta}$ [-] averaged over MOBIDIC's soil depth d . Note that typically, as done in this study, SHAW's total soil depth is more than the depth of the hydrologically active soil layer. Let the superscripts "O", "S" and "M", denote observed, SHAW-simulated, and MOBIDIC-simulated variables, respectively. For SHAW, $\bar{\theta}^S$ (super-script S) is the depth-weighted average of the θ_i values,

$$\bar{\theta}^S = \frac{1}{d} \sum_{i=1}^n \theta_i^S d_i \quad (23)$$

Gravitational and capillary soil moisture dynamics

A. Castillo et al.

Title Page

Abstract

Introduction

Conclusions

References

Tables

Figures

⏪

⏩

◀

▶

Back

Close

Full Screen / Esc

Printer-friendly Version

Interactive Discussion



where, d is the sum of the thickness of each soil layers, d_i [L],

$$d_i = z_{i+1/2} - z_{i-1/2} \quad i = 1, 2, 3, \dots, n. \quad (24)$$

For MOBIDIC, $\overline{\theta^M}$ (super-script M) is the sum of the equivalent depth [L] of water stored in the capillary reservoir W_c^M , the gravity reservoir W_g^M , and the time-invariant residual water content W_r^M , normalized by d ,

$$\overline{\theta^M} = (W_c^M + W_g^M + W_r^M)/d. \quad (25)$$

The soil moisture can also be expressed as equivalent depth,

$$\overline{W^S} = d \overline{\theta^S} \quad (26)$$

$$\overline{W^M} = d \overline{\theta^M}. \quad (27)$$

Moreover, in order to compare with MOBIDIC's partitioning of soil moisture into gravity-water and capillary-bound water, the total water content simulated by SHAW for the i th soil layer is partitioned into gravity water $W_{g,i}^S$, and capillary water $W_{c,i}^S$. Water in excess of the field capacity is considered gravitational storage water, while water between residual water content and field capacity, is considered capillary-bound.

$$W_{g,i}^S = \begin{cases} d_i (\theta_i^S - \theta_{\text{fld},i}^S) & \text{if } \theta_i^S > \theta_{\text{fld},i}^S \\ 0 & \text{if otherwise} \end{cases} \quad (28)$$

$$W_{c,i}^S = \begin{cases} d_i (\theta_{\text{fld},i}^S - \theta_{\text{res},i}^S) & \text{if } \theta_i^S > \theta_{\text{fld},i}^S \\ d_i (\theta_i^S - \theta_{\text{res},i}^S) & \text{if } \theta_{\text{fld},i}^S \geq \theta_i^S > \theta_{\text{res}}^S \\ 0 & \text{if otherwise} \end{cases} \quad (29)$$

By summing over the same soil depth d , the corresponding total water stored in the gravity and capillary reservoirs simulated by SHAW are obtained,

Title Page

Abstract

Introduction

Conclusions

References

Tables

Figures

⏪

⏩

⏴

⏵

Back

Close

Full Screen / Esc

Printer-friendly Version

Interactive Discussion



$$\overline{W_g^S} = \sum_{i=1}^n W_{g,i}^S \quad (30)$$

$$\overline{W_c^S} = \sum_{i=1}^n W_{c,i}^S \quad (31)$$

2.4 Test sites

The comparison is performed using two sites with contrasting climatic regimes. The first site is the “Lucky Hills” catchment in Walnut Gulch Experimental Watershed, Arizona. The climate is semiarid with two-thirds of the annual precipitation occurring during the North American Monsoon from July to September (Goodrich et al., 2008; USDA-ARS, 2007). The site has a mild topography with deep groundwater table. The vegetation is dominated by shrubs (creosote bush or *Larrea tridentata*) with sparse grass (USDA-ARS, 2007). The soil is sandy and gravelly loam. Meteorological data and measurements of soil moisture and temperature are available from the USDA-ARS Southwest Watershed Research source (<http://www.wcc.nrcs.usda.gov>). Soil moisture is measured at seven depths (5, 15, 30, 50, 75, 100, and 200 cm). For consistency, the SHAW model is setup with nine soil nodes with the two extra nodes located at 0 and 300 cm. A subset of the calibrated soil parameters of the SHAW model for this site is shown in Table 2.

The second site is the USDA Soil Climate Analysis Network (SCAN) station “Mayday” in Yazoo, west central Mississippi (32°52′ N, 90°31′ W, elevation 33 m a.s.l.). Located on the Mississippi Delta, this site is characterized by thick clayey alluvial soil, flat topography, shallow groundwater table, and agricultural land use. Its humid subtropical climate is significantly influenced by the warm and moist air often originating from the Gulf of Mexico. In contrast to Site 1, precipitation here is almost evenly distributed throughout the year. Hourly meteorological data and measurements of soil moisture and soil temperature are available from the SCAN source (<http://www.wcc.nrcs.usda.gov/scan>).

Title Page

Abstract

Introduction

Conclusions

References

Tables

Figures

⏪

⏩

◀

▶

Back

Close

Full Screen / Esc

Printer-friendly Version

Interactive Discussion



Soil moisture and temperature are measured at five depths (5, 10, 20, 50, and 100 cm). The SHAW model was setup with eight soil nodes with the three extra nodes located at 0, 75, and 150 cm.

2.5 Calibration

The periods simulated for both sites cover four years with the first being the warm-up period, the second and third as the calibration period, and the last as the validation period. The use of a real-year warm-up period greatly reduces possible errors that can be caused by incorrect initialization of the model.

The strategy is to first focus on the SHAW model. The albedo and the depth-averaged saturated water content of the calibrated SHAW model, are carried over to the 1-D MOBIDIC model. Considering the dynamics of the soil moisture profiles observed at both sites, the soil depth chosen for comparison is the top 50 cm. This is also the soil depth d used for MOBIDIC. With d and $\overline{\theta_{\text{sat}}^M}$ fixed, the remaining parameters to be calibrated to set MOBIDIC's $W_{c,\text{max}}$ and $W_{g,\text{max}}$ are $\overline{\theta_{\text{fld}}^M}$ and $\overline{\theta_{\text{res}}^M}$, recall Eqs. (2) and (3). Once the MOBIDIC model is calibrated, the values of $\overline{\theta_{\text{fld}}^M}$ and $\overline{\theta_{\text{res}}^M}$ are used to calculate SHAW's $\overline{\theta_{\text{fld},i}^S}$ and $\overline{\theta_{\text{res},i}^S}$ for each layer such for $z = 0$ to 50 cm, $\overline{\theta_{\text{fld}}^S} = \overline{\theta_{\text{fld}}^M}$ and $\overline{\theta_{\text{res}}^S} = \overline{\theta_{\text{res}}^M}$. A second set of comparison is done by rerunning the calibrated MOBIDIC model using the same parameters except $d = 30$ cm. The results are also compared against observed and SHAW-simulated values averaged over this depth. Table 3 lists the calibrated soil properties for both the SHAW and MOBIDIC models. For the SHAW layers, the calibrated $\overline{\theta_{\text{sat},i}}$ ranges from 0.19 to 0.21. Although low, these values are as expected because the site is very gravelly and rocky. Also listed are the calibrated capacities of the dual-pore of MOBIDIC and the corresponding soil water contents at saturation, field capacity, and residual content, for the top 50 cm of soil.

Gravitational and capillary soil moisture dynamics

A. Castillo et al.

[Title Page](#)

[Abstract](#)

[Introduction](#)

[Conclusions](#)

[References](#)

[Tables](#)

[Figures](#)



[Back](#)

[Close](#)

[Full Screen / Esc](#)

[Printer-friendly Version](#)

[Interactive Discussion](#)



More importantly, the performance of MOBIDIC in capturing the magnitude range and temporal dynamics of soil moisture, is comparable to that of SHAW. Figure 3 also shows the time series of observed precipitation and the MOBIDIC-simulated ET. High ET occurs around Julian Day 200–300, with a maximum of about 5 mm day^{-1} . For the rest of the year, ET rarely exceeds 0.5 mm day^{-1} . These are realistic values.

To illustrate the adequacy of the dual-pore soil structure of MOBIDIC, the W_c and W_g simulated by MOBIDIC, are plotted against the corresponding values derived from the outputs of SHAW (see Fig. 4a and b). As shown, the two models are in general agreement indicating that the magnitude range and temporal dynamics of MOBIDIC's W_c and W_g have correspondence in SHAW. Two plots are used to highlight the difference in time scale between the capillary-bound and gravity water. Gravity storage is filled during rain storms and it is emptied rapidly. In contrast, capillary-bound water has multi-day time scale in its dynamics with its recession lasting for months.

Using the SHAW and MOBIDIC models calibrated for the top 50 cm, the performance metrics were also evaluated for $z = 0\text{--}30 \text{ cm}$. Table 4 summarizes the results for Site 1. The degradation of model performance in the validation period is minimal. Actually, the performance even improved for soil moisture in the validation period for the top 30 cm.

3.2 Site 2 – Mayday, Mississippi

In contrast to Site 1, this site is sub-humid. Figure 5 shows the soil moisture simulated by SHAW (lines) vs. observations (points). The soil moisture generally increases and becomes more stable with depth indicating the presence of a shallow water table. The soil node at $z = 50 \text{ cm}$ remained practically saturated for the entire simulated period. Overall, the SHAW-simulated θ_i^S at various depths mimic the magnitude range and temporal dynamics of the observations.

Figure 6a plots the time series of observed precipitation and MOBIDIC-simulated ET. After precipitation wetting events, the evapotranspiration rate can be as high as about 12 mm day^{-1} . During the rest of the year, ET is normally $1\text{--}3 \text{ mm day}^{-1}$.

Gravitational and capillary soil moisture dynamics

A. Castillo et al.

Title Page

Abstract

Introduction

Conclusions

References

Tables

Figures



Back

Close

Full Screen / Esc

Printer-friendly Version

Interactive Discussion



Gravitational and capillary soil moisture dynamics

A. Castillo et al.

Title Page

Abstract

Introduction

Conclusions

References

Tables

Figures



Back

Close

Full Screen / Esc

Printer-friendly Version

Interactive Discussion



The two objective measures of goodness-of-fit are evaluated using only the equivalent-depth of water stored in the top 50 cm of soil. For the 2-year calibration period, SHAW performed well ($R = 0.78$, $B = 0.005$) while MOBIDIC performed slightly better ($R = 0.86$, $B = 0.001$), see Fig. 6b. For the validation period, both models significantly underestimate θ . As shown in Fig. 6b, the soil column remained saturated during almost the entire validation period whereas SHAW and MOBIDIC naturally predicted the recession of θ due to ET and drainage. A possible reason for the discrepancy is irrigation in upstream areas, which causes significant lateral subsurface flow and raises the groundwater table, and which is not properly accounted in the two models applied without upstream conditions.

As expected of a site with shallow groundwater table, clayey soil, and sub-humid climate, the soil capillary reservoir remains full during non-drought years, i.e., the soil remains near or above field capacity. The fluctuation of the total soil moisture at this site is associated only with the soil gravity reservoir. Figure 6c shows that the MOBIDIC-simulated $\overline{W_g^S}$ and the equivalent values derived from SHAW, $\overline{W_c^S}$ track one another in both magnitude range and dynamics. Again, this indicates that MOBIDIC's dual-pore soil has behavioral correspondence in the Richards equation based SHAW model.

The values of the performance metrics for soil moisture and temperature for Site 2 are summarized in Table 5. Similar to the findings in Site 1, the results here show that MOBIDIC's simple dual pore storage model captures the essential local scale soil moisture dynamics that is comparable to those simulated with a solver like SHAW. Furthermore, the two models performed relatively better in Site 1 than in Site 2 because the former is well-represented by an independent vertical soil column, whereas in the latter, lateral subsurface fluxes and groundwater interactions are important.

4 Summary

The local scale (referring to vertical discretization of the soil column) in distributed hydrologic models is often modeled using grids with millimeters to centimeters spacing.

Acknowledgements. This research is funded in part by the Singapore National Research Foundation (NRF) through the Singapore-MIT Alliance for Research and Technology (SMART) Center for Environmental Sensing and Monitoring (CENSAM).

References

- 5 Ashby, S. F. and Falgout, R. D.: A parallel multigrid preconditioned conjugate gradient algorithm for groundwater flow simulations, *Nucl. Sci. Eng.*, 124, 145–159, 1996. 7136
- Bartholmes and Todini: Coupling meteorological and hydrological models for flood forecasting, *Hydrol. Earth Syst. Sci.*, 9, 333–346, doi:10.5194/hess-9-333-2005, 2005. 7136
- 10 Beven, K. J.: Linking parameters across scales: subgrid parameterizations and scale dependent hydrological models, *Hydrol. Process.*, 9, 507–525, doi:10.1002/hyp.3360090504, 1995. 7137
- Beven, K. J.: A manifesto for the equifinality thesis, *J. Hydrol.*, 320, 18–36, doi:10.1016/j.jhydrol.2005.07.007, 2006. 7136
- Beven, K. J. and Germann, P.: Macropores and water flow in soils revisited, *Water Resour. Res.*, 49, 3071–3092, doi:10.1002/wrcr.20156, 2013. 7135, 7137
- 15 Beven, K. J. and Kirby, M. J.: A physically based, variable contributing area model of basin hydrology, *Hydrol. Sci. Bull.*, 24, 43–69, doi:10.1080/02626667909491834, 1979. 7135
- Bogaart, P. W., Teuling, A. J., and Troch, P. A.: A state-dependent parameterization of saturated-unsaturated zone interaction, *Water Resour. Res.*, 44, W11423, doi:10.1029/2007WR006487, 2008. 7143
- 20 Brooks, J. R., Barnard, H. R., Coulombe, R., and McDonnell, J. J.: Ecohydrologic separation of water between trees and streams in a Mediterranean climate, *Nat. Geosci.*, 3, 100–104, doi:10.1038/ngeo722, 2009. 7139
- Brooks, R. H. and Corey, A. T.: Hydraulic Properties of Porous Media, Tech. rep., Agricultural Research Service, Soil and Water Conservation Research Division, and the Agricultural Engineering Dept., Colorado State Univ., Fort Collins, Colorado, 1964. 7143
- 25 Burnash, R. J., Ferral, R. L., and McGuire, R. A.: A generalized streamflow simulation system: conceptual models for digital computers, Tech. rep., Joint Federal-State River Forecast Center, Sacramento, CA, 1973. 7135

Gravitational and capillary soil moisture dynamics

A. Castillo et al.

Title Page

Abstract

Introduction

Conclusions

References

Tables

Figures



Back

Close

Full Screen / Esc

Printer-friendly Version

Interactive Discussion



Gravitational and capillary soil moisture dynamics

A. Castillo et al.

[Title Page](#)

[Abstract](#)

[Introduction](#)

[Conclusions](#)

[References](#)

[Tables](#)

[Figures](#)

[⏪](#)

[⏩](#)

[◀](#)

[▶](#)

[Back](#)

[Close](#)

[Full Screen / Esc](#)

[Printer-friendly Version](#)

[Interactive Discussion](#)



- Campo, L., Caparrini, F., and Castelli, F.: Use of multi-platform, multi-temporal remote-sensing data for calibration of a distributed hydrologic model: an application in the Arno Basin, Italy, *Hydrol. Process.*, 20, 2693–2712, doi:10.1002/hyp.6061, 2006. 7141
- Castelli, F., Menduni, G., and Mazzanti, B.: A distributed package for sustainable water management: a case study in the Arno Basin, *International Assoc. of Hydrological Sci. (IAHS) Publ.* 327, IAHS Press, Capri, Italy, 52–61, 2009. 7136, 7140, 7141
- Eagleson, P. S.: Climate, soil, and vegetation 1: Introduction to water balance dynamics, *Water Resour. Res.*, 14, 722–730, doi:10.1029/WR014i005p00705, 1978. 7142, 7143
- Flerchinger, G. N. and Saxton, K. E.: Simultaneous heat and water model of a freezing snow-residue-soil system I. Theory and development, *T. ASAE*, 32, 565–571, 1989. 7145
- Gardner, W. R.: Some steady-state solutions of the unsaturated moisture flow equation with application to evaporation from a water table, *Soil Sci.*, 85, 228–232, 1958. 7143
- Gelhar, L. W., Welty, C., and Wehfeldt, K. R.: A critical review of data on field-scale dispersion in aquifers, *Water Resour. Res.*, 28, 1955–1974, doi:10.1029/92WR00607, 1992. 7137
- Gerke, H. H. and van Genuchten, M. T.: A dual-porosity model for simulating the preferential movement of water and solutes in structured porous media, *Water Resour. Res.*, 29, 305–319, doi:10.1029/92WR02339, 1993. 7138
- Goodrich, D. C., Keefer, T. O., Unkrich, C. L., Nichols, M. H., Osborn, H. B., Stone, J. J., and Smith, J. R.: Long-term precipitation database, Walnut Gulch Experimental Watershed, Arizona, United States, *Water Resour. Res.*, 44, W05S04, doi:10.1029/2006WR005782, 2008. 7148
- Harter, T. and Hopmans, J. W.: Role of vadose-zone flow processes in regional-scale hydrology: review, opportunities and challenges, in: *Unsaturated-Zone Modeling: Progress, Challenges and Applications*, Kluwer Academic Publishers, Dordrecht, the Netherlands, 179–208, 2004. 7135, 7137
- Ivanov, V. Y., Vivoni, E. R., Bras, R. L., and Entekhabi, D.: Catchment hydrologic response with a fully distributed irregular network model, *Water Resour. Res.*, 40, W11102, doi:10.1029/2004WR003218, 2004. 7136
- Ivanov, V. Y., Fatichi, S., Jenerette, G. D., Espeleta, J. F., Troch, P. A., and Huxman, T. E.: Hysteresis of soil moisture spatial heterogeneity and the homogenizing effect of vegetation, *Water Resour. Res.*, 46, W09521, doi:10.1029/2009WR008611, 2010. 7135

Gravitational and capillary soil moisture dynamics

A. Castillo et al.

[Title Page](#)

[Abstract](#)

[Introduction](#)

[Conclusions](#)

[References](#)

[Tables](#)

[Figures](#)

[⏪](#)

[⏩](#)

[◀](#)

[▶](#)

[Back](#)

[Close](#)

[Full Screen / Esc](#)

[Printer-friendly Version](#)

[Interactive Discussion](#)



- Kollet, S. J., Maxwell, R. M., Woodward, C. S., Smith, S., Vanderborght, J., Vereecken, H., and Clemens, S.: Proof of concept of regional scale hydrologic simulations at hydrologic resolution utilizing massively parallel computer resources, *Water Resour. Res.*, 46, W04201, doi:10.1029/2009WR008730, 2010. 7137
- 5 Larsbo, M., Roulier, S., Stenemo, F., Kasteel, R., and Jarvis, N.: An improved dual-permeability model of water flow and solute transport in the vadose zone, *Vadose Zone J.*, 4, 398–406, doi:10.2136/vzj2004.0137, 2005. 7138
- Lawrence, J. E. and Hornberger, G. M.: Soil moisture variability across climate zones, *Geophys. Res. Lett.*, 34, L20402, doi:10.1029/2007GL031382, 2007. 7135
- 10 Liu, M., Bárdossy, A., Li, J., and Jiang, Y.: Physically-based modeling of topographic effects on spatial evapotranspiration and soil moisture patterns through radiation and wind, *Hydrol. Earth Syst. Sci.*, 16, 357–373, doi:10.5194/hess-16-357-2012, 2012. 7135
- McDonnell, J. J.: The two water worlds hypothesis: ecohydrological separation of water between streams and trees?, *WIREs Water*, doi:10.1002/wat2.1027, in press, 2014. 7139
- 15 Qu, Y. and Duffy, C. J.: A semidiscrete finite volume formulation for multiprocess watershed simulation, *Water Resour. Res.*, 43, W08419, doi:10.1029/2006WR005752, 2007. 7136
- Rawls, W. J., Brakensiek, D. L., and Saxton, K. E.: Estimation of soil water properties, T. ASCE, ASAE Paper No. 81-2510, 1316–1321, 1982. 7141
- Refsgaard, J. C. and Storm, B.: *Computer Models of Watershed Hydrology*, Water Resources Publications, Rome, Italy, 809–846, 1995. 7136
- 20 Rubin, Y.: *Applied Stochastic Hydrogeology*, Oxford University Press, Oxford, UK, 2003. 7137
- Salvucci, G. D.: An approximate solution for steady vertical flux of moisture through an unsaturated homogenous soil, *Water Resour. Res.*, 29, 3749–3753, doi:10.1029/93WR02068, 1993. 7143
- 25 Šimůnek, J. and van Genuchten, M. T.: Modeling non-equilibrium flow and transport processes using HYDRUS, *Vadose Zone J.*, 7, 782–797, doi:10.2136/vzj2007.0074, 2008. 7138
- Smith, S., Seo, D. J., Koren, V. I., Reed, S. M., Zhang, Z., Duan, Q., Moreda, F., and Cong, S.: The Distributed Model Intercomparison Project (DMIP): motivation and experiment design, *J. Hydrol.*, 298, 4–26, doi:10.1016/j.jhydrol.2004.03.031, 2004. 7136
- 30 Smith, S., Koren, V. I., Reed, S. M., Zhang, Z., Zhang, Y., Moreda, F., Cui, Z., Misukami, N., Anderseon, E. A., and Cosgrove, B. A.: The Distributed Model Intercomparison Project – Phase 2: motivation and design of the Oklahoma experiments, *J. Hydrol.*, 418–419, 3–16, doi:10.1016/j.jhydrol.2011.08.056, 2012. 7136

Gravitational and
capillary soil
moisture dynamics

A. Castillo et al.

Table 2. Calibrated soil properties of the SHAW model of Site 1. b and ψ_e are the Campbell pore-size distribution index, and air-entry potential, respectively.

z cm	b –	ψ_e cm	K_s mm h^{-1}	ρ kg m^{-3}	θ_{sat} –	sand %	silt %	clay %	OM %
0	5.8	–100	11.0	1380	0.19	63	22	15	1.0
5	6.1	–120	10.0	1380	0.20	63	22	15	0.6
15	6.1	–150	6.00	1380	0.20	63	22	15	0.5
30	6.1	–200	3.00	1380	0.20	62	22	16	0.4
50	6.5	–220	0.50	1420	0.21	62	22	16	0.3
75	9.0	–300	0.35	1450	0.21	54	21	25	0.2
100	9.5	–300	0.30	1600	0.20	53	22	25	0.1
200	10.0	–300	0.25	1600	0.19	52	22	26	0.0
300	10.0	–300	0.25	1600	0.19	50	22	28	0.0

Title Page

Abstract

Introduction

Conclusions

References

Tables

Figures

◀

▶

◀

▶

Back

Close

Full Screen / Esc

Printer-friendly Version

Interactive Discussion



Gravitational and capillary soil moisture dynamics

A. Castillo et al.

Table 4. Performance of the SHAW and MOBIDIC models of Site 1 for the calibration period (year 2007 and 2008) and validation period (year 2009).

	Depth	Calibration		Validation	
		<i>R</i>	<i>B</i>	<i>R</i>	<i>B</i>
<i>Soil Moisture</i>					
SHAW	0–50	0.89	0.018	0.83	0.034
MOBIDIC	0–50	0.88	0.023	0.84	0.016
SHAW	0–30	0.86	0.059	0.95	0.001
MOBIDIC	0–30	0.86	0.019	0.87	0.022
<i>Soil Temperature</i>					
SHAW	Z_d	0.98	0.017	0.98	0.023
MOBIDIC	Z_d	0.93	0.074	0.93	0.059

[Title Page](#)
[Abstract](#)
[Introduction](#)
[Conclusions](#)
[References](#)
[Tables](#)
[Figures](#)
[Back](#)
[Close](#)
[Full Screen / Esc](#)
[Printer-friendly Version](#)
[Interactive Discussion](#)


Gravitational and capillary soil moisture dynamics

A. Castillo et al.

Table 5. Performance of the SHAW and MOBIDIC models of Site 2 for the calibration period (water year 2006 and 2007) and validation period (water year 2008).

	Depth	Calibration		Validation	
		<i>R</i>	<i>B</i>	<i>R</i>	<i>B</i>
<i>Soil Moisture</i>					
SHAW	0–50	0.78	0.005	0.34	0.050
MOBIDIC	0–50	0.86	0.001	0.46	0.045
SHAW	0–30	0.79	0.007	0.42	0.065
MOBIDIC	0–30	0.82	0.049	0.51	0.013
<i>Soil Temperature</i>					
SHAW	Z_d	0.93	0.232	0.92	0.219
MOBIDIC	Z_d	0.95	0.001	0.94	0.009

Title Page

Abstract

Introduction

Conclusions

References

Tables

Figures

◀

▶

◀

▶

Back

Close

Full Screen / Esc

Printer-friendly Version

Interactive Discussion



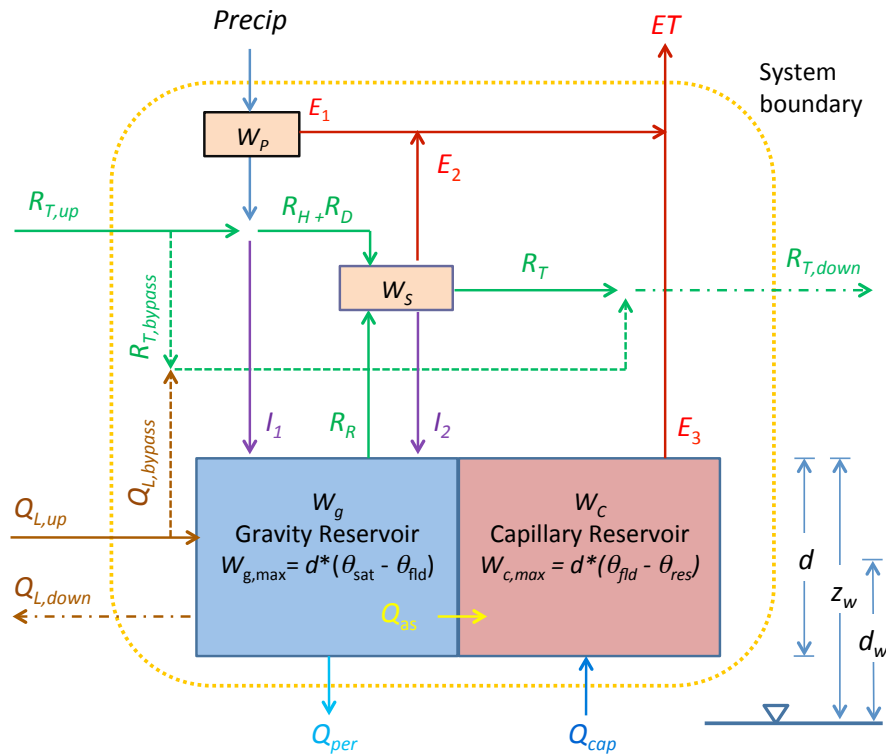


Figure 1. Schematic diagram of MOBIDIC's mass balance at each soil unit.

Title Page	
Abstract	Introduction
Conclusions	References
Tables	Figures
◀	▶
◀	▶
Back	Close
Full Screen / Esc	
Printer-friendly Version	
Interactive Discussion	



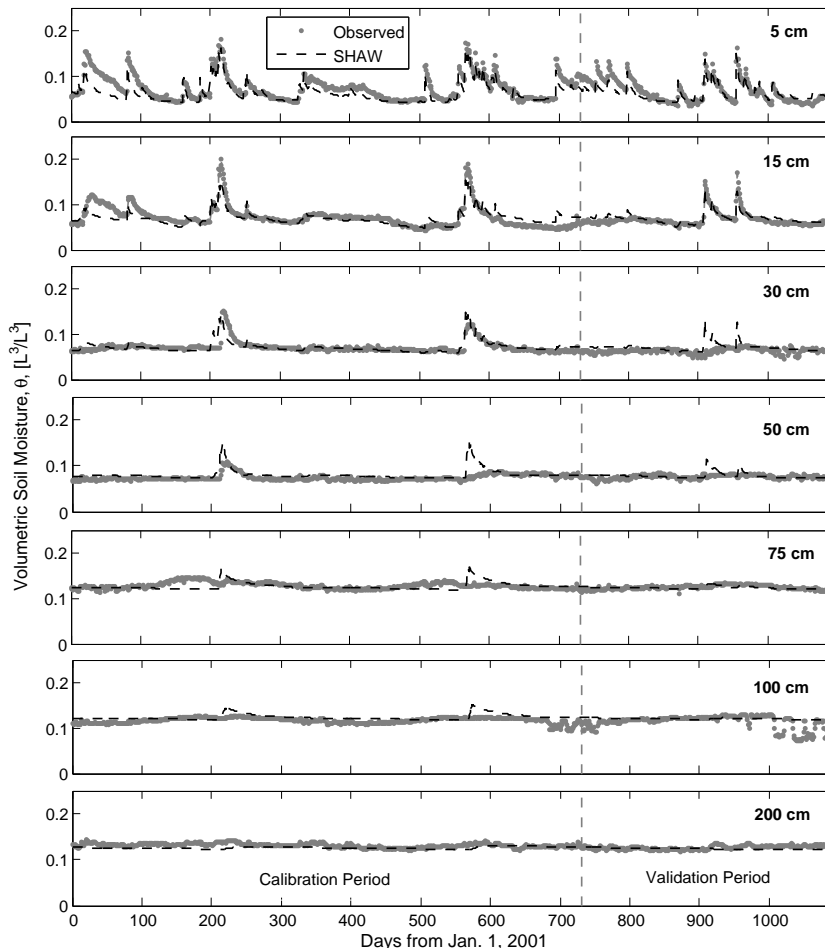


Figure 2. Observed vs. SHAW-simulated volumetric soil moisture [$L^3 L^{-3}$] at Site 1.

Gravitational and capillary soil moisture dynamics

A. Castillo et al.

[Title Page](#)

[Abstract](#) [Introduction](#)

[Conclusions](#) [References](#)

[Tables](#) [Figures](#)

[◀](#) [▶](#)

[◀](#) [▶](#)

[Back](#) [Close](#)

[Full Screen / Esc](#)

[Printer-friendly Version](#)

[Interactive Discussion](#)



Gravitational and
capillary soil
moisture dynamics

A. Castillo et al.

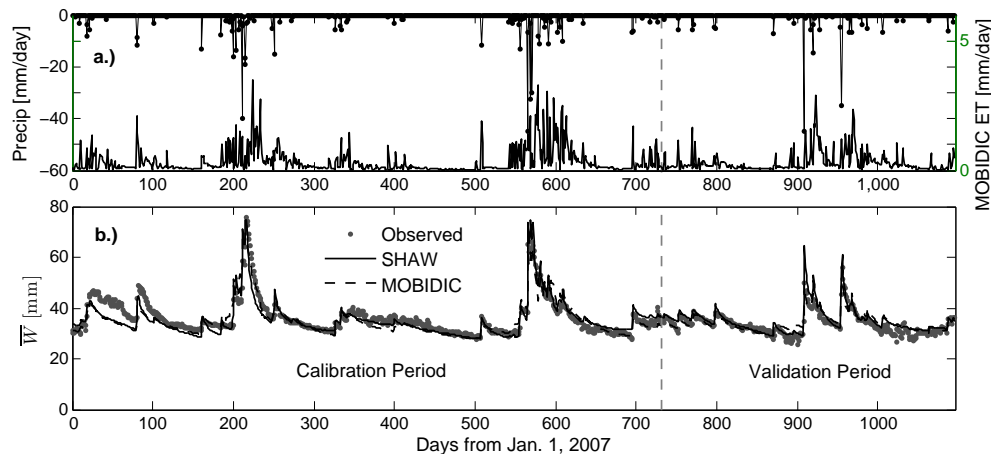


Figure 3. (a) Observed precipitation [mm day^{-1}] and MOBIDIC-simulated ET [mm day^{-1}]; (b) observed equivalent depth [cm] of soil water stored in the top 50 cm vs. corresponding values simulated by SHAW and MOBIDIC for Site 1.

Title Page

Abstract

Introduction

Conclusions

References

Tables

Figures

◀

▶

◀

▶

Back

Close

Full Screen / Esc

Printer-friendly Version

Interactive Discussion



Gravitational and capillary soil moisture dynamics

A. Castillo et al.

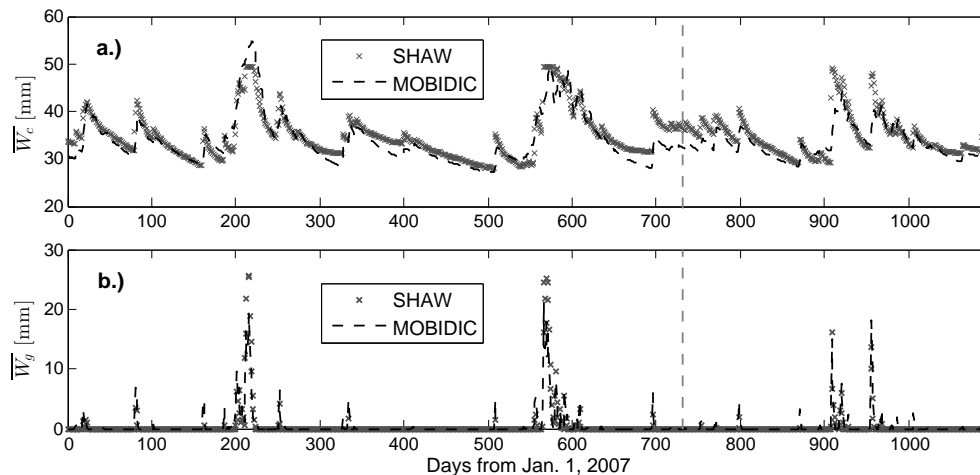


Figure 4. The SHAW- and MOBIDIC-simulated equivalent depth [cm] of water stored in the soil (a) capillary reservoir; and (b) gravity reservoir, for the top 50 cm of Site 1.

[Title Page](#)[Abstract](#)[Introduction](#)[Conclusions](#)[References](#)[Tables](#)[Figures](#)[Back](#)[Close](#)[Full Screen / Esc](#)[Printer-friendly Version](#)[Interactive Discussion](#)

Gravitational and capillary soil moisture dynamics

A. Castillo et al.

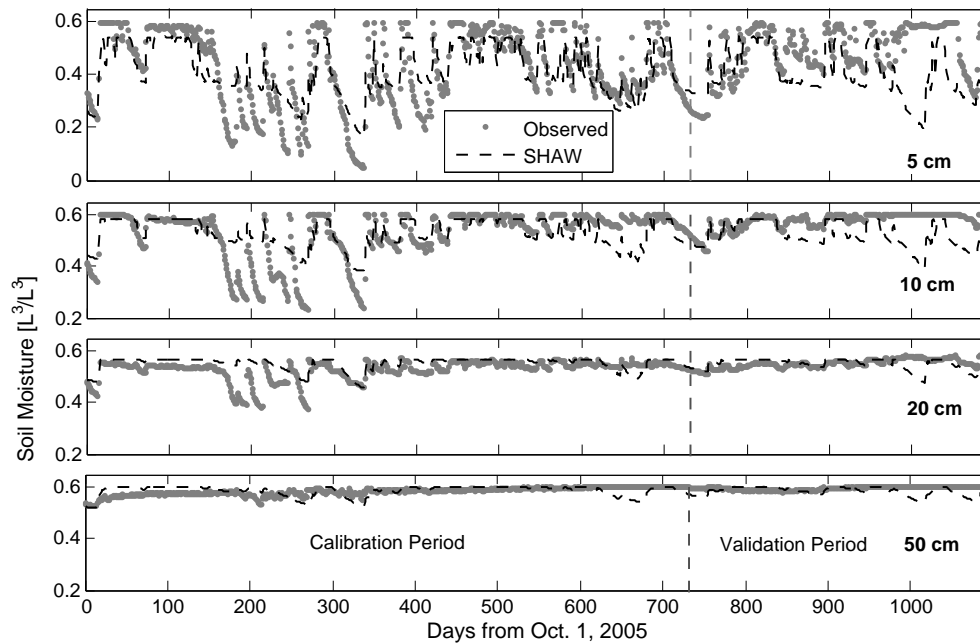


Figure 5. Observed vs. SHAW-simulated volumetric soil moisture [L^3L^{-3}] at Site 2.

[Title Page](#)[Abstract](#)[Introduction](#)[Conclusions](#)[References](#)[Tables](#)[Figures](#)[Back](#)[Close](#)[Full Screen / Esc](#)[Printer-friendly Version](#)[Interactive Discussion](#)

Gravitational and capillary soil moisture dynamics

A. Castillo et al.

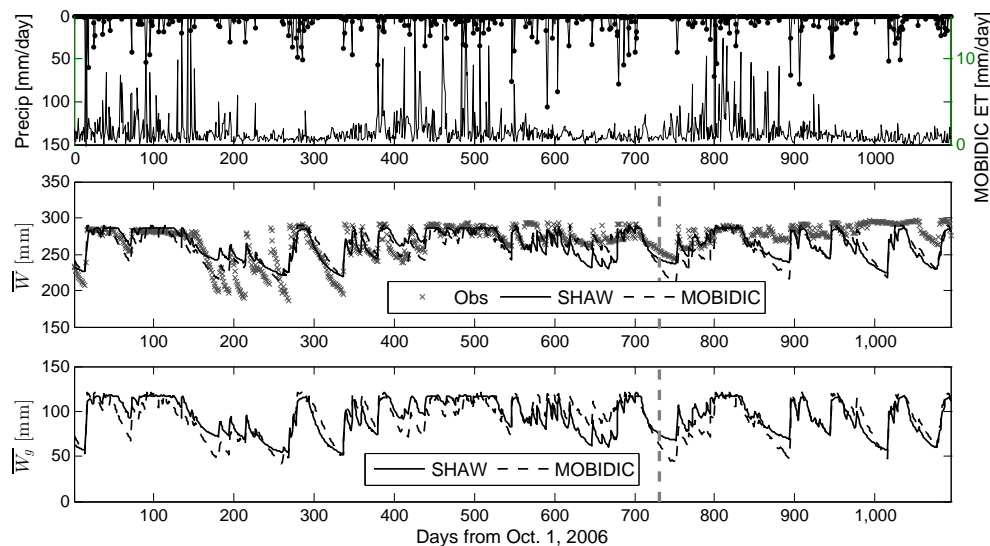


Figure 6. For Site 2: **(a)** observed precipitation [mm day^{-1}] and MOBIDIC-simulated ET [mm day^{-1}]; **(b)** observed, SHAW-, and MOBIDIC-simulated equivalent depth [mm] of soil water stored in the top 50 cm; and **(c)** MOBIDIC- and SHAW-simulated equivalent depth [mm] of water in the capillary reservoir of the top 50 cm of soil.

[Title Page](#)
[Abstract](#)
[Introduction](#)
[Conclusions](#)
[References](#)
[Tables](#)
[Figures](#)

[Back](#)
[Close](#)
[Full Screen / Esc](#)
[Printer-friendly Version](#)
[Interactive Discussion](#)
